

Glcci1 Deficiency Leads to Proteinuria

Yukino Nishibori,* Kan Katayama,* Matalena Parikka,* Ásmundur Oddsson,* Masatoshi Nukui,* Kjell Hultenby,[†] Annika Wernerson,[†] Bing He,* Lwaki Ebarasi,* Elisabeth Raschperger,* Jenny Norlin,* Mathias Uhlén,[‡] Jaakko Patrakka,* Christer Betsholtz,* and Karl Tryggvason*

*Department of Medical Biochemistry and Biophysics, Division of Matrix Biology, Karolinska Institutet, Stockholm, Sweden; [†]Department of Laboratory Medicine, Division of Pathology, Karolinska Institutet, Stockholm, Sweden; and [‡]Department of Biotechnology, Royal Institute of Technology, Stockholm, Sweden

ABSTRACT

Unbiased transcriptome profiling and functional genomics approaches identified glucocorticoid-induced transcript 1 (*GLCCI1*) as being a transcript highly specific for the glomerulus, but its role in glomerular development and disease is unknown. Here, we report that mouse glomeruli express far greater amounts of *Glcci1* protein compared with the rest of the kidney. RT-PCR and Western blotting demonstrated that mouse glomerular *Glcci1* is approximately 60 kD and localizes to the cytoplasm of podocytes in mature glomeruli. In the fetal kidney, intense *Glcci1* expression occurs at the capillary-loop stage of glomerular development. Using gene knockdown in zebrafish with morpholinos, morphants lacking *Glcci1* function had collapsed glomeruli with foot-process effacement. Permeability studies of the glomerular filtration barrier in these zebrafish morphants demonstrated a disruption of the selective glomerular permeability filter. Taken together, these data suggest that *Glcci1* promotes the normal development and maintenance of podocyte structure and function.

J Am Soc Nephrol 22: 2037–2046, 2011. doi: 10.1681/ASN.2010111147

The glomerular filtration barrier consists of three layers: fenestrated endothelial cells, glomerular basement membrane (GBM), and podocyte foot processes with their interconnecting slit diaphragm.^{1,2} Damage to this filter system can lead to proteinuria, development of nephrotic syndrome, and consequent ESRD if the disease process cannot be reversed. Glomerular filter injury can be caused by mutations in genes of functional importance for the glomerular cells or the GBM,² or it is acquired, e.g. via chemical lesions. About 60% of all ESRD cases in the United States initiate as glomerular insults, the main cause being diabetes mellitus.³ Regardless of etiology, the glomerular injury manifests itself initially as proteinuria that may or may not progress to ESRD. Although there may be different causes for protein leakage into the urinary space, there are clearly several different molecular pathomechanisms, but to date there is little knowledge about the details of most processes involved in proteinuria development.

Several podocyte proteins associated with the slit-diaphragm region have been of great interest from the point of view of their role in the filter function, as well as in as in proteinuria disease processes.² However, it is apparent that a number of other proteins are involved in different forms of glomerular disease. We have applied an unbiased transcriptome profiling and functional genomics approach in attempt to identify proteins that are highly specific for glomerular cells and extracellular matrix structures and that thus

Received November 10, 2010. Accepted July 7, 2011.

Published online ahead of print. Publication date available at www.jasn.org.

Correspondence: Dr. Karl Tryggvason, Department of Medical Biochemistry and Biophysics, Division of Matrix Biology, Karolinska Institutet, 171 77 Stockholm, Sweden. Phone: 46-8-524-87720; Fax: 46-8-316-165; E-mail: karl.tryggvason@ki.se

Copyright © 2011 by the American Society of Nephrology

might play roles in glomerular development and disease.^{4–6} Analysis of mouse glomeruli led to the identification of >300 novel transcripts of unknown function with highly glomerulus-specific expression in the kidney. Polyclonal antibodies have been generated to a large number of these proteins, and expression and distribution of several of the novel glomerulus-associated proteins were reported.⁷ However, the biologic roles of those and many other glomerular proteins are still unknown.

One of the highly glomerulus-specific transcripts identified in our screen encodes glucocorticoid induced transcript 1 (*GLCCI1*, ENSMUSG0000029638), which is expressed 14-fold higher in the glomerulus than in the rest of kidney and 2.8-fold higher in podocytes than in other glomerular cells.⁴ *Glcci1* has previously been described as a thymocyte-specific transcript that is rapidly up-regulated in response to dexamethasone treatment⁸ and represents early response in steroid-regulated thymocyte apoptosis.⁹ Mouse *Glcci1* is located in the cytoplasm of T cells, and the RNA is highly expressed in thymus and testis but very weakly expressed in all of the other tissues studied, including kidney. In humans, *Glcci1* expression has also been reported to be mainly restricted to thymus and testis¹⁰ and also as a phosphorylated protein in mouse brain cells.¹¹ In developmental studies, expression of this gene has been shown in the somites and presomitic mesoderm.^{12,13} However, its overall biologic role and potential function in the kidney are still unknown.

Recently, zebrafish has been utilized as a screening system for protein function in kidney development.^{14,15} In zebrafish, the pronephros consists of a single glomerulus with pronephric tubules on each side. The pronephric glomerular filtration barrier with its fenestrated endothelial cells, GBM, and podocytes is very similar to that in mammals, including humans, and it develops into a functional filtration unit between 36 and 48 hours postfertilization (hpf).¹⁴ In fact, the zebrafish pronephros has been shown to be an excellent model to study function of glomerular proteins, by disrupting RNA translation or pre-mRNA splicing using antisense oligonucleotides. Defects in glomerular filtration can be analyzed using an *in vivo* filtration assay¹⁴ or by a new method developed in this study for analyzing excreted urine proteins. Thus, nephrin or podocin knock-down zebrafish morphants exhibit a loss of slit diaphragm and passage of macromolecular FITC-dextran into the tubule and duct lumen as described previously.¹⁵

In this study, we have studied the effects of *Glcci1* knock-down on zebrafish pronephros and shown that it causes proteinuria and morphologic changes in the filtration barrier, indicating that this protein may be involved in pathogenic mechanisms of glomerular disease.

RESULTS

Expression of *Glcci1* in Mouse Kidney

The high glomerular expression of *Glcci1* observed in our previous mouse glomerular transcriptome analysis⁴ was confirmed here in both mouse and human kidneys. By reverse transcription (RT)-PCR from different mouse cDNA libraries, the highest expression was observed in testis, brain, and thymus, but there was also high expression in lymph nodes, spleen, and eye. In contrast, very weak signal was observed in total kidney RNA (Figure 1A). However, glomerular RNA displayed high expression compared with the rest of the kidney. Northern-blot analysis revealed the highest expression in thymus and testis, whereas little if any expression was observed whole-kidney RNA (Figure 1B). The mRNA in thymus had two major bands of 5.0 and 6.0 kb, whereas the testis mRNA was of the size of 2.0 kb, suggesting alternatively spliced variants, essentially as described previously.¹⁰ Western blotting revealed a single

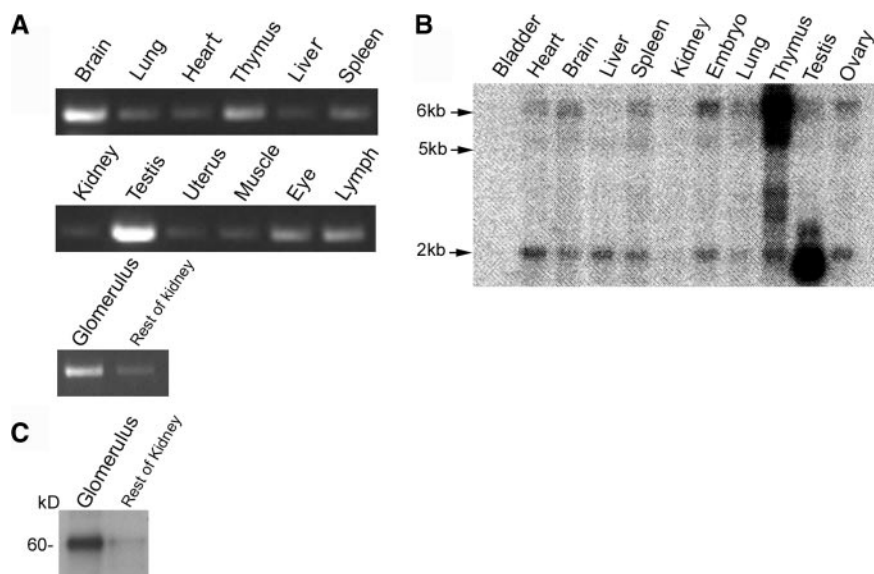


Figure 1. Expression of *Glcci1* in mouse organs reveals varying tissue expression and strong upregulation in kidney glomeruli. (A) Using RT-PCR, high expression is seen in testis, brain, and thymus; somewhat lower expression is seen in lymph nodes, spleen, and eye; and weak signals are seen in lung, heart, liver, muscle, uterus, and whole kidney. However, RT-PCR of RNA from isolated glomeruli gives a strong signal compared with that in RNA from the rest of the kidney. (B) Northern blot reveals strong expression of mRNAs of 5.0 and 6.0 kb in the thymus and of about 2.0-kb-size mRNA in testis. The other organs reveal weak signals for both the 2.0- and 6.0-kb mRNAs. (C) Western blotting of protein extracted from isolated glomeruli show a strong single band of about 60 kD and a weak staining of same size protein in the rest of the kidney.

strong band with a molecular mass of about 60 kD in protein extract from isolated mouse glomeruli, and a similar size weak band was observed in protein extract from kidney tissue devoid of glomeruli (Figure 1C). As shown in Figure 2, the Glcc1 antibody exhibited clear immunoreactivity in glomeruli, Glcc1 being mainly expressed in podocytes but also in mesangial cells (Figure 2, B and C). The staining was observed in the cytoplasm, which is consistent with an intracellular protein. Immunoelectron microscopy performed on normal mouse (Figure 2D) and rat kidneys showed a similar distribution. Semiquantification showed the following distribution of gold particles in defined areas: 57% in podocytes, 35% in the mesangium, 5% in endothelial cells, and 3% in the GBM. During normal mouse development, Glcc1 was observed in podocyte cytoplasm at capillary-loop stage at embryonic day 15.5, but not at the earlier S-shaped stage of glomeruli. These findings show that Glcc1 is expressed late in mouse podocyte development (Fig. 3).

Dexamethasone Induces Glcc1 Expression in Cultured Mouse Podocytes and Isolated Glomeruli

Because the expression of Glcc1 mRNA is induced by glucocorticoid in mouse thymocytes,^{8,9} we investigated whether dexamethasone (DEX) also induces its expression in mouse podocytes. As shown in Figure 4A, incubation with 0.01, 0.1, and 1 μ M DEX for 12 hours revealed in-

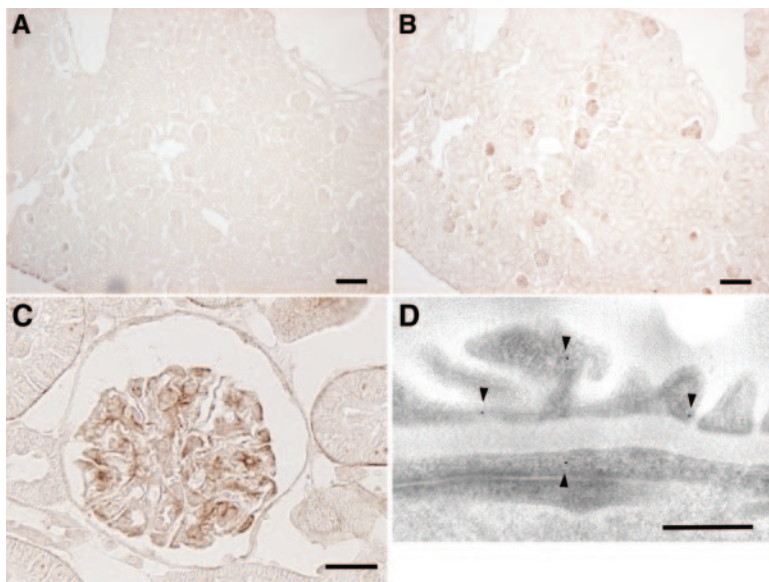


Figure 2. Kidney GLCCI1 expression is restricted to podocytes and mesangial cells. Paraffin sections of adult mouse kidney cortex were immunostained with the polyclonal anti-human GLCCI1 antibody or rabbit IgG (5 μ g/ml) as control. (A) No immunoreactivity was observed in adjacent specimens immunostained with normal rabbit IgG. (B) Low power magnification reveals immunoreactivity exclusively in glomeruli of the mouse kidney cortex. (C) At higher magnification, immunostaining of the glomerular podocytes and mesangium with strong cytoplasm staining is apparent. Magnifications: $\times 100$ in overviews and $\times 800$ in single glomeruli. (D) Immunogold labeling in normal mouse capillaries shows the majority of gold particles to be located in the podocyte foot processes. Bars, A and B, 100 μ m; C, 10 μ m; and D, 0.5 μ m.

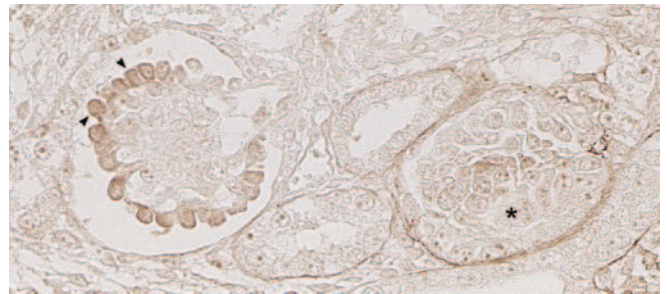


Figure 3. GLCCI1 is expressed in capillary state but insignificantly in earlier S-shape glomeruli. Immunostaining of GLCCI1 in fetal mouse kidney shows expression at embryonic day 15.5. GLCCI1 is initially expressed in podocyte cytoplasm (arrowheads) of capillary loop stage glomerulus. At the earlier S-shape stage (asterisk), GLCCI1 expression is insignificant.

creased expression, the highest being observed at 1 μ M on the basis of RT-PCR analysis. To examine whether this induction is mediated through binding to the glucocorticoid receptor (GR), we studied whether the glucocorticoid antagonist RU486 could block the DEX-mediated induction. Here, mouse podocytes were pretreated with 0.01 μ M of RU486 for 30 minutes before addition of DEX to a final concentration of 0.1 μ M. The Glcc1 expression in cultured podocyte was induced with increasing DEX concentration and significantly reduced under RU486 treatment (Figure 4A). We then studied Glcc1 expression in glomeruli isolated from control mice and mice treated with DEX (2 mg/kg injection) for 12 hours. Figure 4B shows that Glcc1 mRNA was increased in DEX-treated mouse glomeruli. The expression of Glcc1 mRNA increased by about 40% by DEX treatment under these conditions, indicating that is mediated through binding to GR.

Expression of Glcc1 in Zebrafish

Sequence identity between zebrafish and human Glcc1 is 53% at the amino-acid level (Supplementary Figure 1) and 54% at the nucleotide level. This sequence identity is sufficient to perform comparative expression, as well as functional analysis in zebrafish. To study the expression of Glcc1 in zebrafish, we analyzed RT-PCR and immunostaining. As shown in Figure 5A, RT-PCR analysis revealed strong expression of the Glcc1 transcript in total embryonic RNA at 3 hpf, after which is dropped significantly during 6 to 24 hours and then increased again to quite a steady level during 48 to 168 hpf. By immunostaining, Glcc1 is also observed in the glomeruli in a cross-section

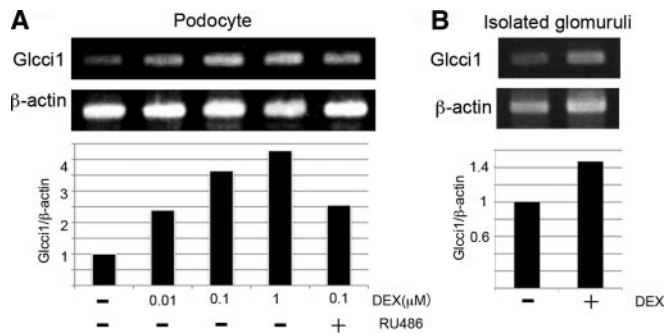


Figure 4. Dexamethasone induces expression of *Glc11* in mouse podocytes and glomeruli. RT-PCR for *Glc11* and β -actin (internal standard) expression was carried out on total RNA isolated from DEX-treated cultured mouse podocytes and glomeruli isolated from mice treated with DEX. (A) Podocytes were cultured at different DEX concentrations, and in one case with the GR antagonist RU486 for 30 minutes before the addition of DEX. (B) Expression in glomeruli isolated from mice treated with DEX (2 mg/kg) for 12 hours. Histograms show an increase in *Glc11* expression after DEX treatment.

through the zebrafish pronephros at 144 hpf (Figure 5, C and D). To verify these results, we dissected under UV-light single glomeruli from embryos of a zebrafish line expressing green fluorescent protein under the podocin promoter,¹⁶ isolated total RNA, and carried out RT-PCR for *Glc11* expression. The results shown in Figure 5E demonstrated strong expression of *Glc11* as well as of nephrin in the isolated glomeruli, whereas the rest of the fish devoid of glomeruli had a considerably lower average expression. Taken together, these results demonstrate *Glc11* expression in the glomeruli of zebrafish larvae.

Interference of *Glc11* Function with Antisense Morpholino Oligos

To get insight into the possible importance of *Glc11* for zebrafish pronephric development and function, we targeted this gene with antisense morpholino oligos (MOs). MOs were designed against the splice acceptor (ex2A MO) and donor (ex2D MO) sites on exon 2 in the *Glc11* transcript, as well as for the translation initiation site. MO injection resulted in missplicing of mRNA for the gene, as detected by sequence of altered RT-PCR products (Figure 6A). The sequence of altered *glc11* mRNA revealed an insertion of part of intron 2 and a deletion of exon 2, both of which caused premature stop codon after frameshifts (Figure 6B). Morphant embryos injected with MOs targeting the acceptor and donor sites developed clear cardiac edema, dorsal body axis curvature, and short stature (Figure 6C) in 79% of the *glc11* ex2D MO. Morphant embryos injected with MOs targeting the translation start site (trans) also caused cardiac edema and short stature, but not as severe dorsal body curvature (data not shown). The embryos were terminated by age of 6 days. The phenotype suggests wide effects, including a functional disorder of the pronephros. Embryos injected with standard controls did not exhibit edema

and bent tail and appeared as wild type. To establish specificity of the MO effects, we determined whether *glc11* morphant phenotypes could be rescued by coinjection of a synthetic zebrafish *glc11* mRNA. The embryos that were coinjected with *glc11* MO and zebrafish *glc11* mRNA were morphologically normal in terms of cardiac edema and axis curvature in 96% of coinjected embryos compared with 22% of *glc11* MO. (Figure

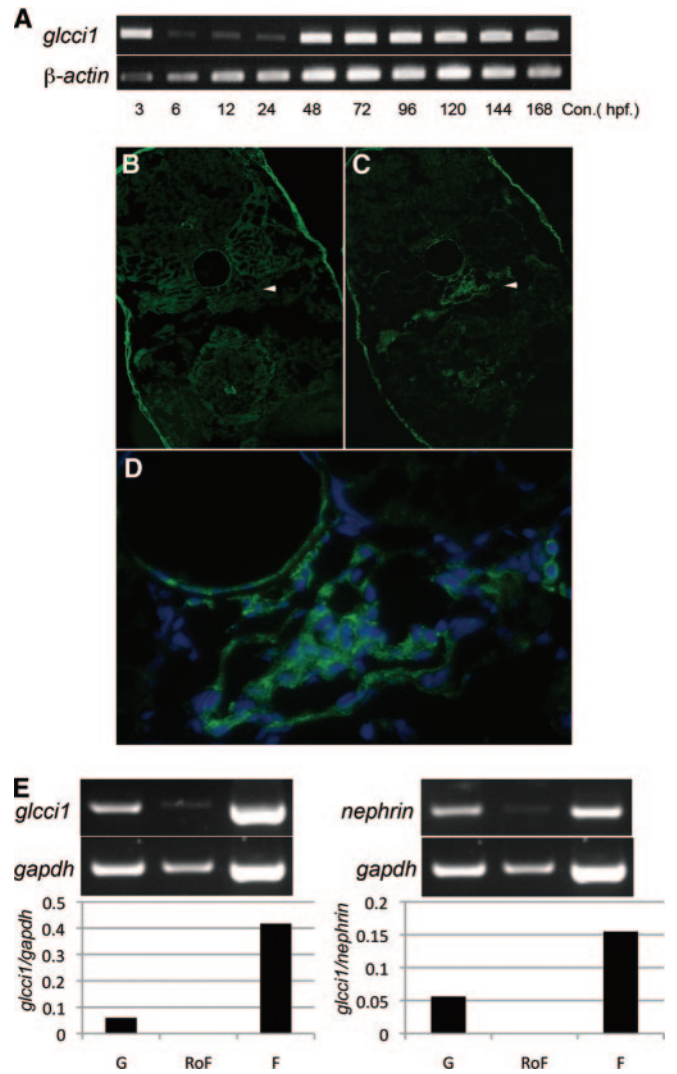


Figure 5. GLCCI1 is expressed in podocytes and mesangial cells in the zebrafish pronephros. (A) RT-PCR was performed on total embryonic RNA at 3, 6, 9, and 12 hpf, and at days 1 to 7 postfertilization. *glc11* mRNA is detected in whole zebrafish embryos. β -actin is a housekeeping gene known to be expressed in early development of zebrafish. (B) Immunohistochemistry shows negative staining for Glc11 in the glomerulus with control rabbit IgG. (C) Immunohistochemistry shows positive staining for Glc11 expression in the zebrafish pronephros (arrowheads) (original magnification, $\times 20$). (D) At higher magnification, immunostaining of cytoplasm and a mesangium-like pattern are visible. (E) RT-PCR of RNA isolated from single zebrafish embryo glomeruli demonstrates distinct expression of *glc11*. G, glomeruli; RoF, rest of fish; F, whole zebrafish.



Figure 6. Disruption of *glcci1* expression with splice donor antisense MOs causes pericardial edema, short stature, and curved body axis. The efficacy of the injected MO was compared by RT-PCR. (A) *glcci1* MO targeting the exon 2 splice donor caused an insertion of part of intron 2 and a deletion of exon 2. (B) The changes in amplified RNA fragments are seen as a decrease in amplicon size (375 bp versus 530 bp) as illustrated here by amino acid sequences that are aligned in the panel or as a nonsplicing of adjacent intron, visible as an increase in amplicon size (567 bp) caused by a truncation after a stretch of nonsense amino acids. (C) Compared with wild-type embryos, *glcci1* MO larvae develop severe cardiac edema and bent tail at 96 hpf. (D) Rescue of the *glcci1* MO phenotype with zebrafish *glcci1* mRNA coinjection. Coinjection with 100 pg of zebrafish *glcci1* mRNA completely rescued the phenotype (97%).

6D). The data indicate that the effects of the splice and translation blocking MOs are specific to the *glcci1* mRNA. Histologic sections of embryos showed the pronephros to exhibit

dilated capillary loop structures and expanded Bowman's space compared with wild type (Figure 7, A and B). These findings were detected in 48-hpf *glcci1* morphants. Transmission electron microscopy was carried out on pronephros in wild-type and *glcci1* morphants zebrafish to explore effects of malfunctional *glcci1* mRNA on glomerular capillaries (Figure 7, C and D). Indeed, the morphant podocytes exhibited normal glomerular basement membrane and endothelial cells compared with wild type. The morphology of the podocytes and their foot processes were heterogeneous. Areas with foot-process effacement dominated, but normal areas with intact slit membranes were also found.

Dextran dye filtration assay has been used previously to investigate a failure of filtration barrier in zebrafish.^{14,17} We also examined 500- and 70-kD dye filtration assay with *glcci1* MO, but the dye dextran did not appear to leak to pronephric ducts where it could be partially reabsorbed. To explore whether the pronephric macromolecular barrier function was compromised in *glcci1* morphants, we analyzed for excretion of proteins in the zebrafish embryos using a novel method developed in this study. Instead of using intravenously injected dye dextrans that have been used to monitor macromolecular leakage in zebrafish glomeruli, we collected and concentrated the water from small petri dishes containing wild-type and morphant embryos and analyzed them for protein content using SDS-PAGE. As shown in Figure 7E, interference of the synthesis of Glcci1 protein and nephrin in zebrafish embryos clearly resulted in the leakage of proteins of a similar size as bovine albumin as well as an about 150-kD component as the main components in the urine of *glcci1* morphants, whereas uninjected WT or in control morphants did not excrete any protein. The two main fractions of about 70 and 150 kD were isolated by SDS-PAGE and subjected to sequencing by mass spectrometry analysis, and both bands contained as the main components zebrafish vitellogenin, a transport protein highly abundant in the yolk and in blood of zebrafish (Supplementary Table 1). In adult zebrafish serum, the main component of about 70 kD was shown to be transferrin, but vitellogenin was still also abundant (Supplementary Table 2). In adult zebrafish serum, vitellogenin was the main component of the 150-kD fraction (Supplementary Table 2). We conclude that the new method is effective for examining proteinuria phenotype in zebrafish.

Glcci1 Expression of Glomerular Disease Models in Mice

Because reduced production of Glcci1 leads to proteinuria in zebrafish embryos, we studied glomerular expression of the *Glcci1* gene in three mouse models of glomerular disease: adriamycin nephrosis, LPS nephrosis, and db/db model for diabetic nephropathy. The *Glcci1* expression was indeed significantly downregulated in all of these models for proteinuria. *Glcci1* was decreased to 23% ($P < 0.0095$) in the adriamycin model (Nukui M, He L, Patrakka J, Takemoto M, Betsholtz C, Tegnér J, Tryggvason K, manuscript in preparation), to 33% in the LPS model¹⁸, and to 77% ($P < 0.03$) in a db/db diabetic

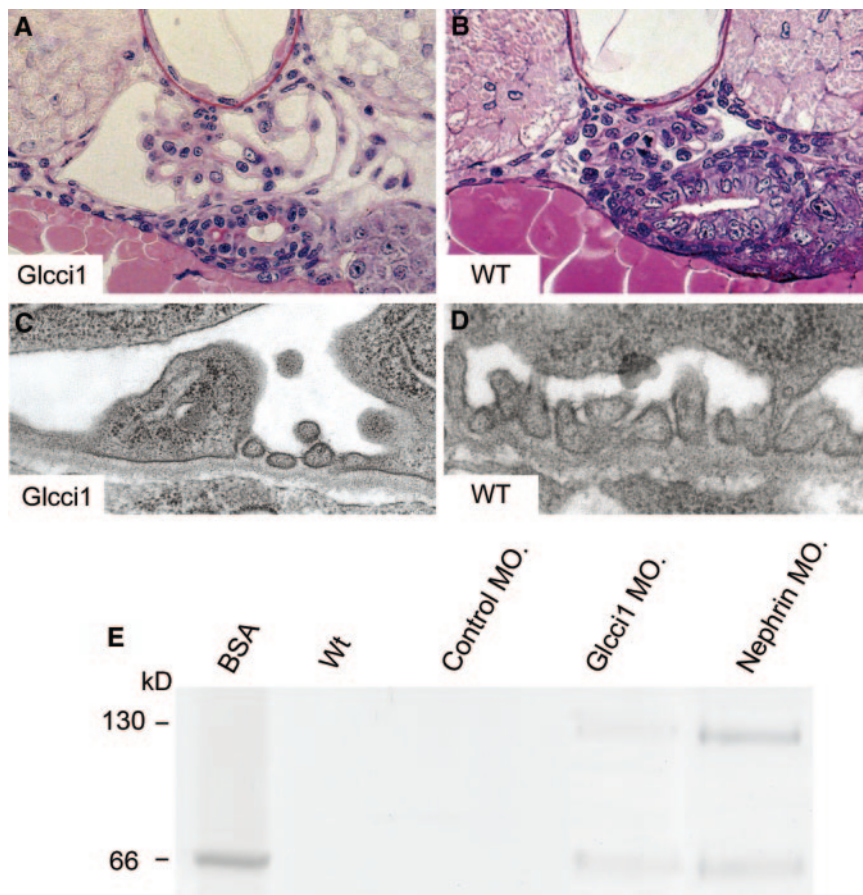


Figure 7. Disruption of *glcci1* expression causes abnormal glomerular capillary loops, podocyte effacement, and proteinuria. (A and B) In light microscopy, Periodic acid-Schiff staining shows dilated capillary loops and widened Bowman's space (A) compared with wild type (B). (C and D) In *glcci1* knockdown embryos, the foot processes are largely lost because of effacement, but normal areas with intact slit membranes were also observed (C). Ultrastructural studies show normal podocyte foot processes, glomerular basement membrane, and endothelial cells in wild-type embryos (D). (E) Not only nephrin knockdown embryos but also *glcci1* knockdown embryos develop proteinuria that can be observed by SDS-PAGE analysis. The main protein penetrating the filtration barrier was identified by mass spectrometry analysis as vitellogenin that has a size of about 150 and 70 kD, of the same size as BSA that primarily appears to be a degradation product of vitellogenin.

nephropathy model (Norlin J, He L, Tryggvason K, Betsholtz C, manuscript in preparation). These analyses may indicate that *Glcci1* is quite generally downregulated in podocyte injury leading to proteinuria.

DISCUSSION

We have previously characterized the glomerular transcriptome in mouse as part of our efforts to identify proteins of importance for the development and function of glomeruli, as well as to characterize genes and proteins involved in the poorly understood molecular processes of glomerular disease.^{4–6} *Glcci1* was one of the transcripts very strongly ex-

pressed in isolated mouse glomeruli, the expression being 14-fold that of the rest of the kidney. Such an intense glomerulus-specific expression pattern in the kidney suggested that *GLCCI1* has a significant role in the glomerulus. Here we showed that *GLCCI1* expression starts at the capillary-loop stage in mouse podocytes when the podocytes start to develop foot processes. The slit-diaphragm-specific proteins nephrin and podocin are also expressed in podocytes first at the capillary-loop stage.^{19,20} Many podocyte-specific proteins are involved in slit-diaphragm formation, cell-cycle regulation, and terminal differentiation of the podocyte lineage at this stage,²¹ so *GLCCI1* is likely to be required for renal development and maturation. *glcci1* expression was also significant at 48 hpf when the pronephros develops into a function filtration unit in the zebrafish embryo (Figure 5). On the other hand, *glcci1* was also expressed in early embryonic development at 3 hpf, whereas the expression decreased from 6 to 24 hpf.

To explore the biologic role of *Glcci1*, we decided to use zebrafish as a model for such *in vivo* studies. Zebrafish is an excellent species for studies on renal development and pathophysiology because of its rapid ex utero development, optical transparency, and possibilities for gene manipulation. *glcci1* has previously been reported to be expressed at ~36 to 48 hpf of zebrafish, but it has not been studied in kidney development.²² Because *Glcci1* was shown here by RT-PCR and immunostaining analyses to be strongly expressed in the single embryonic zebrafish glomerulus of the pronephros, which is functional already at 48 hpf, the zebrafish was an excellent

model to study the potential developmental importance of *Glcci1*. Indeed, the results of these MOs knockdown experiments showed that *Glcci1*-deficient embryos developed a rather severe phenotype with cardiac edema, short stature, frequent dorsal axis curvature, and death before 1 week of age. A partially similar phenotype has previously been shown for nephrin and podocin gene knockdown zebrafish.¹⁵ These effects were clearly specific, because they could be prevented with coinjection of splice-blocking MO and zebrafish *glcci1* mRNA. Whereas the *glcci1* knockdown clearly caused extrarenal abnormalities, there were also distinct pathologic changes in the pronephric kidneys of *Glcci1* knockdown zebrafish embryos, *i.e.* poor development of glomerular capillaries and expanded Bowman's capsule. The electron microscopy analyses

also demonstrated irregular and often enlarged podocyte foot processes, demonstrating that *Glcc1* is important for proper development of the foot processes as well as regional thickening and lamellation of the GBM. Analyses for the presence of protein in the urine demonstrated that glomerular filtration was compromised in *glcc1* knockdown embryos. We consider the zebrafish proteinuria assay developed here more appropriate than the use of exogenous and intravenously injected 70- and 500-kD size dyed dextrans, because it does not require any injections of unphysiological macromolecules. For example, it has been reported that even 500-kD dextrans can normally escape the glomerular filtration barrier because of the linear shape of dextrans.²³

The results of this study demonstrating a role for the *Glcc1* protein in glomerular development and function in zebrafish can be of interest from the point of view of human glomerular diseases. The molecular pathomechanisms of glomerular diseases in humans are generally poorly understood, and there appear to be many pathogenic molecular pathways initiating a glomerular disease that progresses to a common phenotype at advanced stage with extensive proteinuria, injury of podocytes and other glomerular cells, eventual glomerulosclerosis, and glomerular collapse. Because of the poor understanding of molecular disease mechanisms, it has been difficult to develop novel drugs for glomerular disease. However, steroids have long belonged to the repertoire of main drugs used in the treatment of a large number of kidney diseases. The finding of a highly glomerulus-specific steroid-sensitive gene/protein was intriguing. Because we have previously carried out glomerulus-specific transcriptome profiling in mice with LPS nephrosis¹⁸ and adriamycin-induced nephrosis and diabetic nephropathy in db/db mice (Norlin J, He L, Tryggvason K, Betsholtz C, manuscript in preparation), we also checked the expression of *Glcc1* in the glomeruli in these models. As described above, *Glcc1* expression was significantly decreased in all of these three models, *i.e.* –33% in LPS nephrosis, 23% in ADR-induced nephrosis, and as much as 77% in db/db nephropathy. It was therefore of interest to explore whether treatment of these mice with steroids would induce expression of *Glcc1* and possibly even have a therapeutic effect. However, glucocorticoid treatment of mice with ADR-induced nephropathy, with irreversible focal segmental glomerulosclerosis like phenotype, did not have any effects on glomerular *Glcc1* expression levels or any therapeutic effects (Nukui M, He L, Patrakka J, Takemoto M, Betsholtz C, Tegnér J, Tryggvason K, manuscript in preparation). The involvement of *Glcc1* in steroid-responsive treatment remains to be shown, and therefore, it will be interesting to study the expression and involvement of *Glcc1* in other mouse models or glucocorticoid-responsive human glomerular disease.

In conclusion, this study has shown that expression of the zebrafish podocyte *Glcc1* protein is essential for proper maturation of podocyte properly and maintenance of the glomerulus capillary structure and podocyte function. However, it is still unclear how GLCC1 possible affects

podocyte disease or which role the regulation of GLCC1 may have in kidney disease.

CONCISE METHODS

Antibodies

For generation of polyclonal antibodies against human GLCC1, a 280- to 419-amino acid protein was expressed as recombinant proteins with a dual tag: a hexahistidine tag that enabled purification of the expressed antigen by immobilized metal ion affinity chromatography and an albumin-binding protein fragment of *Streptococcus* protein G with immunopotentiating capabilities.²⁴ Antibodies were raised by immunization of NZW rabbits, and the obtained sera were used for purification of monospecific antibodies. Purification was performed using a two-step purification procedure including depletion of tag-specific antibodies and subsequent affinity purification as described previously.²⁵ The following antibodies were purchased from the suppliers as indicated: Horseradish peroxidase-labeled goat anti-rabbit IgG (Dako, Carpinteria, CA), Alexa Fluor 488-conjugated goat anti-rabbit IgG (Molecular Probes, Eugene, OR), and 4',6'-diamino-2-phenylindole (Molecular Probes).

Reverse Transcriptase-Polymerase Chain Reaction and Northern Blot

Expression of *Glcc1* in different mouse tissues was studied using RT-PCR and Northern Blots. Primer sequences and sizes were *Glcc1* forward 5'-AATCCCAGGATGGAGTCCT-3', reverse 5'-GCTCCCTCTGCTTTAGAT-3'; 538 bp, β -actin forward 5'-GAC-AACGGCTCCGGCATGTGCA-3', reverse 5'-ATGACCTGGCCGT-CAGGCAGCT-3'. As a template for PCR analysis, we used cDNA libraries that were generated from various adult mouse tissues (Mouse Multiple Tissue cDNA Panel; Clontech Laboratories, Palo Alto, CA). Total RNA was extracted from whole mouse kidney, isolated glomeruli, and immortalized mouse podocyte (a gift from Dr Peter Mundel, Mount Sinai School of Medicine, New York, NY). Glomeruli were isolated from adult ICR outbred mice (Charles River Laboratories, Wilmington, MA) by means of a magnet beads perfusion method.²⁶ PCR amplification was carried out with long PCR enzyme (Fermentas International Inc., Burlington, Canada) under the following conditions: 31 cycles at 94°C for 30 seconds, 55°C for 1 minute, and 72°C for 1 minute. The PCR products were analyzed by electrophoresis on 1% agarose gels.

To study expression of *glcc1* in zebrafish, we extracted total RNA from whole zebrafish embryos using TRIzol (Invitrogen) and amplified the RNA using RT-PCR. *glcc1* cDNA was amplified using oligonucleotide primers: forward 5'-AGCACAGGTGCTATCAGACG-3', reverse 5'-GTCAGGGCAGGAGAAAAGTG-3'; β -actin forward 5'-CGAGCAGGAGATGGGAACC-3', reverse 5'-AGAGCAGAAGC-CATGCTGAT-3'. RT-PCR primers were designed from flanking exon coding sequence to confirm morpholino-oligo efficacy and characterize the altered mRNA splicing products using following primers: *glcc1* ex2F5'-CTGCCCTCATTACCTGTC-3' and *glcc1* ex2R5'-TCTCCAGTCCATGGTTGATG-3'.

For Northern blots, PCR products obtained from the amplifica-

tion of cDNA libraries (see previous paragraph) were used as templates to create ^{32}P -labeled probes using the Rediprime II random primer labeling system (Amersham Pharmacia Biotech, London, UK). Probes were hybridized to FirstChoice Northern Blot Mouse Blot I (Ambion, Huntington, UK) using recommended wash solutions and Ultrahyb hybridization solution according to the manufacturer's instructions.

Hybridizations also were performed on blots that contained mRNA that was isolated from mouse kidney fractions that contained either only kidney glomeruli or the kidney excluding glomeruli. Glomerular fractions were isolated as described previously.⁴ The hybridizations were performed as described above. A mouse *Gapdh3* probe (Clontech Laboratories) was used as a loading control.

Western Blotting

In Western blotting, we used protein extracts of highly purified mouse glomeruli, as well as the remaining kidney tissue devoid of glomeruli. The highly pure glomeruli were isolated from 8- to 12-week-old adult mice as described previously.²⁶ The samples were separated by NuPAGE 4 to 12% Bis-Tris gel (Invitrogen, Carlsbad, CA) electrophoresis. They were then transferred to polyvinylidene difluoride membranes and incubated overnight at 4 °C with anti-Glcc1 antibody (1:4000). The filter was then incubated for 1 hour at room temperature with an horseradish peroxidase-labeled donkey anti-rabbit antibody and developed by using an ECL advanced western blotting kit (Amersham) according to the manufacturer's instructions.

Zebrafish Lines

Zebrafish were grown and mated following standard protocols. The wild-type lines and transgenic line expressing green fluorescent protein under the zebrafish podocin promoter¹⁶ were from an AB strain zebrafish (*Danio rerio*). Dechorionated embryos were kept at 28°C in E3 solution with or without 0.003% 1-phenyl-2-thiourea (Sigma, St. Louis, MO) to suppress pigmentation and staged according to somite number or hpf.

Immunohistochemistry

For immunostaining, adult mouse kidney samples were collected from 6-week-old male ICR mice (26–28 g; Saitama Experimental Animals Supply Co., Ltd., Sugito, Saitama, Japan) that were anesthetized by intraperitoneal injection with pentobarbital. Mouse embryonic kidneys were collected at embryonic day 15.5 during gestation. Samples of mouse kidneys were fixed in 10% formaldehyde in PBS for 6 hours at 4°C and embedded in paraffin wax, and 4- μm sections were made. The slides were de-waxed, washed with PBS, and autoclave-heated at 120°C for 10 minutes in Target Retrieval Solution (Dako) for antigen retrieval. After incubation with 1% H_2O_2 /PBS for 30 minutes and washing with PBS, the slides were incubated with blocking buffer (3% BSA, 5% goat serum, and 0.05% Tween-20 in PBS) for 60 minutes and then reacted with anti-Glcc1 polyclonal antibody (1:50) or rabbit IgG (5 $\mu\text{g}/\text{ml}$) for 2 hours at room temperature. After washing with PBS, the slides were incubated at room temperature with horseradish peroxidase-labeled goat anti-rabbit antibody (1:100) and then developed by immersion in 1.4 mM 3,3'-diaminobenzidine tetrahydrochloride (Sigma) in PBS.

For immunofluorescence staining of zebrafish, whole 144-hpf wild-type embryos were snap-frozen, and cryosections (5 μm) were postfixed with cold acetone for 10 minutes, followed by blocking in 3% bovine serum albumin. The primary anti-GLCCI1 antibody (1:50) or normal rabbit IgG were incubated overnight at 4°C, followed by 1 hour of incubation with a secondary antibody. Microscopy was performed with standard a Leica fluorescence microscope.

For zebrafish histology analysis, whole embryos were fixed in Bouin's fixative (Polyscience Inc., Warrington, PA), and embedded in glycolmethacrylate (JB-4 resin; Polyscience, Inc.), and serial sectioning was performed on a microtome. Section thickness was approximately 3 μm . The sections were stained with a modified Periodic acid-Schiff staining and examined in a light microscope.

Transmission Electron Microscopy and Immunoelectron Microscopy

For immunoelectron microscopy, tissues from mouse kidney were dehydrated in methanol and embedded in Lowicryl K11M (ProSci Tech, Kirwan, Queensland, Australia). Ultrathin sections were mounted on carbon/Formvar nickel grids and incubated in 2% BSA and 2% gelatin in 0.1 M phosphate buffer at pH 7.4 followed by incubation overnight with anti-Glcc1 antibodies, diluted 1:20 in 0.1 M phosphate buffer containing 0.1% BSA and 0.1% gelatin (PBBG). Bound antibodies were detected by protein A conjugated with 10-nm colloidal gold (Biocell Laboratories Inc., Rancho Dominguez, CA), diluted 1:100 in PBBG. Sections were examined in a Tecnai 10 microscope (FEI Company, Eindhoven, The Netherlands). Digital images were taken by Megaview III (SiS Company, Münster, Germany).

Semiquantification was based on calculation of 25 randomly taken images in the capillaries and 5 images in the mesangium. In the capillaries, gold particles in the endothelium, in the GBM, and within a distance of 2 μm from the GBM on the epithelial side were counted. In the mesangium, gold particles in the mesangial matrix were counted.

Zebrafish embryos were fixed in 2% glutaraldehyde and 0.5% paraformaldehyde in 0.1 M sodium cacodylate buffer containing 0.1 M sucrose and 3 mM CaCl_2 , pH 7.4, at room temperature for 30 minutes, followed by 24 hours at 4°C. The specimens were rinsed in 0.15 M sodium cacodylate buffer containing 3mM CaCl_2 , pH 7.4, postfixed in 2% osmium tetroxide in 0.07 M sodium cacodylate buffer containing 1.5 mM CaCl_2 , pH 7.4, at 4°C for 2 hours, dehydrated in ethanol followed by acetone and embedded in LX-112 (Ladd, Burlington, VT). Semithin sections were made and stained with toluidine blue and used for light microscopic analysis. Ultrathin section were prepared and contrasted with uranyl acetate, followed by lead citrate and examined in a Tecnai 10 transmission electron microscope at 80 kV (FEI Company). Digital images were made using a MegaView III digital camera (Soft Imaging System, GmbH, Münster, Germany).

Morpholino Antisense Oligonucleotides and mRNA Injection

Wild-type embryos (AB) at the one- to two-cell stage were microinjected with 0.15 mM antisense morpholino oligos (Gene Tools, Philomath, OR) in 200 mM KCl and 0.2% Phenol red. Final antisense morpholino oligo concentration in the yolk sac was estimated to be 100 nM.

The splice acceptor site blocking oligonucleotide sequence was *glci1* MOex2A 5'-CTTTGACCTCTCCACTGCTATAAGG-3' and the splice donor site blocking oligonucleotide sequence was *glci1* MOex2D 5'-GTGTAGATTTTGTAGCCTACCTGTGT-3'. The nephrin antisense oligonucleotide was nephrin MO 5'-CGCTGTCCAT-TACCTTTCAGGCTCC-3'.

A standard control oligonucleotide 5'-cctcttacctcagtacaattata-3' showed no effect on embryonic development. mRNA rescue experiments were carried out by coinjecting 100 pg of *in vitro* transcribed zebrafish *glci1* mRNA (Message Machine kit; Ambion, Austin, TX) with the morpholino oligo. A full-length *glci1* cDNA was amplified by RT-PCR from zebrafish total RNA using oligonucleotide primers (5'-GGAATTCAGTTGCGTATTTT-3' and 5'-GTCAGGGCAG-GAGAAAAGTG-3') on the basis of the zebrafish *glci1* sequence (ENS DARG0000008503) and subcloned with a TA cloning kit (Invitrogen, Carlsbad, CA). The phenotype of more than 100 embryos that were injected with *glci1* MOex2D, *glci1* MOex2D with *glci1* mRNA, and standard control oligonucleotide were examined and classified with wild-type and anomaly at 96 hpf.

New Method for Assessing Proteinuria in Zebrafish Embryos

A new method was developed to assess the amount of proteinuria in zebrafish embryos. For each measurement, 100 wild-type, control, nephrin MO, and *glci1* MO embryos (AB) were collected at 96 hpf and kept in tanks with 5 ml of fresh E3 water for 24 hours at 28.5°C after changing E3 water twice. At 120 hpf, 4 ml of E3 water were harvested after ensuring that all embryos were alive. One ml of 100% TCA solution, was mixed gently with the tank water and kept at 4°C for 1 hour. The samples were then centrifuged at 13,000 rpm at 4°C for 5 minutes, and the supernatant was removed. The pellets were washed with cold acetone and centrifuged at 13,000 rpm at 4°C for 5 minutes twice. After drying the pellets, 15 μ l of 2 \times NuPAGE LDS sample buffer (Invitrogen) was added and incubated at 70 °C for 10 minutes. For SDS-PAGE, the samples were applied to NuPAGE 4 to 12% Bis-Tris Gels (Invitrogen). Then the gels were stained with Page-Blue Protein Staining Solution (Fermentas International Inc.) and examined for the presence of protein.

Gene Expression Profiling with Affymetrix

Three mouse glomerular disease models were included in this analysis. They are adriamycin-induced mice nephrotic syndrome model (Nukui M, He L, Patrakka J, Takemoto M, Betsholtz C, Tegnér J, Tryggvason K, manuscript in preparation), LPS-induced mice nephrotic syndrome model,¹⁸ and Type II diabetic mice model (Norlin J, He L, Tryggvason K, Betsholtz C, manuscript in preparation). The mouse glomerular RNA was isolated and hybridized on Affymetrix arrays respectively, and the array data were processed as described before.^{5,6}

Ethical Considerations

This study was approved by the ethical committees of the Karolinska Institute.

ACKNOWLEDGMENTS

We are grateful to Susan Warner, Ulla Wargh, and Sajila Kisana at the Karolinska Institute fish facility for their assistance with this work. This study was supported in part by grants from the Knut and Alice Wallenberg's Foundation (to K.T., C.B., and M.U.), the Swedish Foundation for Strategic Research (to K.T. and C.B.), Swedish Medical Research Council (to K.T. and C.B.), the Novo Nordisk Foundation (to K.T. and C.B.), Söderberg's Foundation (to K.T.), Wenner Gren Foundation (to K.K.), the Academy of Finland (to M.P.), Stockholm County Council, the Swedish Association of Kidney Patients, Stig and Gunborg Westman's Foundation, Magnus Bergvall's Foundation (J.P., A.W., and K.H.), as well as the Swedish Association for Medical Research (E.R.).

DISCLOSURES

None.

REFERENCES

- Farquhar MG, Wissig SL, Palade GE: Glomerular permeability: I. Ferritin transfer across the normal glomerular capillary wall. *J Exp Med* 113: 47–66, 1961
- Tryggvason K, Patrakka J, Wartiovaara J: Hereditary proteinuria syndromes and mechanisms of proteinuria. *N Engl J Med* 354: 1387–1401, 2006
- U.S. Renal Data System, USRDS 2008 Annual Data Report: Atlas of Chronic Kidney Disease and End-Stage Renal Disease in the United States, National Institutes of Health, National Institute of Diabetes and Digestive and Kidney Diseases, Bethesda, MD, 2008
- Takemoto M, He L, Norlin J, Patrakka J, Xiao Z, Petrova T, Bondjers C, Asp J, Wallgard E, Sun Y, Samuelsson T, Mostad P, Lundin S, Miura N, Sado Y, Alitalo K, Quaggin SE, Tryggvason K, Betsholtz C: Large-scale identification of genes implicated in kidney glomerulus development and function. *EMBO J* 25: 1160–1174, 2006
- He L, Sun Y, Patrakka J, Mostad P, Norlin J, Xiao Z, Andrae J, Tryggvason K, Samuelsson T, Betsholtz C, Takemoto M: Glomerulus-specific mRNA transcripts and proteins identified through kidney expressed sequence tag database analysis. *Kidney Int* 71: 889–900, 2007
- He L, Sun Y, Takemoto M, Norlin J, Tryggvason K, Samuelsson T, Betsholtz C: The glomerular transcriptome and a predicted protein-protein interaction network. *J Am Soc Nephrol* 19: 260–268, 2008
- Patrakka J, Xiao Z, Nukui M, Takemoto M, He L, Oddsson A, Perisic L, Kaukinen A, Szgyarto CA, Uhlen M, Jalanko H, Betsholtz C, Tryggvason K: Expression and subcellular distribution of novel glomerulus-associated proteins dendrin, ehd3, sh2d4a, plekh2, and 2310066E14Rik. *J Am Soc Nephrol* 18: 689–697, 2007
- Chapman MS, Qu N, Pascoe S, Chen WX, Apostol C, Gordon D, Miesfeld RL: Isolation of differentially expressed sequence tags from steroid-responsive cells using mRNA differential display. *Mol Cell Endocrinol* 108: R1–R7, 1995
- Chapman MS, Askew DJ, Kuscuoğlu U, Miesfeld RL: Transcriptional control of steroid-regulated apoptosis in murine thymoma cells. *Mol Endocrinol* 10: 967–978, 1996
- Miazek A, Malissen B: Two genes, three messengers: Hybrid transcript between a gene expressed at specific stages of T-cell and sperm maturation and an unrelated adjacent gene. *Immunogenetics* 54: 681–692, 2003

11. Munton RP, Tweedie-Cullen R, Livingstone-Zatchej M, Weinandy F, Waidelich M, Longo D, Gehrig P, Potthast F, Rutishauser D, Gerrits B, Panse C, Schlapbach R, Mansuy IM: Qualitative and quantitative analyses of protein phosphorylation in naive and stimulated mouse synaptosomal preparations. *Mol Cell Proteomics* 6: 283–293, 2007
12. Ishikawa A, Kitajima S, Takahashi Y, Kokubo H, Kanno J, Inoue T, Saga Y: Mouse Nkd1, a Wnt antagonist, exhibits oscillatory gene expression in the PSM under the control of Notch signaling. *Mech Dev* 121: 1443–1453, 2004
13. William DA, Saitta B, Gibson JD, Traas J, Markov V, Gonzalez DM, Sewell W, Anderson DM, Pratt SC, Rappaport EF, Kusumi K: Identification of oscillatory genes in somitogenesis from functional genomic analysis of a human mesenchymal stem cell model. *Dev Biol* 305: 172–186, 2007
14. Drummond IA, Majumdar A, Hentschel H, Elger M, Solnica-Krezel L, Schier AF, Neuhauss SC, Stemple DL, Zwartkruis F, Rangini Z, Driever W, Fishman MC: Early development of the zebrafish pronephros and analysis of mutations affecting pronephric function. *Development* 125: 4655–4667, 1998
15. Kramer-Zucker AG, Wiessner S, Jensen AM, Drummond IA: Organization of the pronephric filtration apparatus in zebrafish requires Nephricin, Podocin and the FERM domain protein Mosaic eyes. *Dev Biol* 285: 316–329, 2005
16. He B, Ebarasi L, Hulthenby K, Tryggvason K, Betsholtz C: Podocin-green fluorescence protein allows visualization and functional analysis of podocytes. *J Am Soc Nephrol* 22: 1019–1023, 2011
17. Ebarasi L, He L, Hulthenby K, Takemoto M, Betsholtz C, Tryggvason K, Majumdar A: A reverse genetic screen in the zebrafish identifies crb2b as a regulator of the glomerular filtration barrier. *Dev Biol* 334: 1–9, 2009
18. Sun Y, He L, Takemoto M, Patrakka J, Pikkarainen T, Genove G, Norlin J, Truve K, Tryggvason K, Betsholtz C: Glomerular transcriptome changes associated with lipopolysaccharide-induced proteinuria. *Am J Nephrol* 29: 558–570, 2009
19. Holzman LB, St. John PL, Kovari IA, Verma R, Holthofer H, Abrahamson DR: Nephricin localizes to the slit pore of the glomerular epithelial cell. *Kidney Int* 56: 1481–1491, 1999
20. Roselli S, Gribouval O, Boute N, Sich M, Benessy F, Attie T, Gubler MC, Antignac C: Podocin localizes in the kidney to the slit diaphragm area. *Am J Pathol* 160: 131–139, 2002
21. Nagata M, Nakayama K, Terada Y, Hoshi S, Watanabe T: Cell cycle regulation and differentiation in the human podocyte lineage. *Am J Pathol* 153: 1511–1520, 1998
22. Galloway JL, Wingert RA, Thisse C, Thisse B, Zon LI: Combinatorial regulation of novel erythroid gene expression in zebrafish. *Exp Hematol* 36: 424–432, 2008
23. Zhou X, Vize PD: Proximo-distal specialization of epithelial transport processes within the *Xenopus* pronephric kidney tubules. *Dev Biol* 271: 322–338, 2004
24. Agaton C, Galli J, Hoiden Guthenberg I, Janzon L, Hansson M, Asplund A, Brundell E, Lindberg S, Ruthberg I, Wester K, Wurtz D, Hoog C, Lundberg J, Stahl S, Ponten F, Uhlen M: Affinity proteomics for systematic protein profiling of chromosome 21 gene products in human tissues. *Mol Cell Proteomics* 2: 405–414, 2003
25. Nilsson P, Paavilainen L, Larsson K, Odling J, Sundberg M, Andersson AC, Kampf C, Persson A, Al-Khalili Szigyarto C, Ottosson J, Bjorling E, Hober S, Wernerus H, Wester K, Ponten F, Uhlen M: Towards a human proteome atlas: high-throughput generation of mono-specific antibodies for tissue profiling. *Proteomics* 5: 4327–4337, 2005
26. Takemoto M, Asker N, Gerhardt H, Lundkvist A, Johansson BR, Saito Y, Betsholtz C: A new method for large scale isolation of kidney glomeruli from mice. *Am J Pathol* 161: 799–805, 2002

See related editorial, "Fishing for New Glomerular Disease-Related Genes," on pages 1960–1962.

Supplemental information for this article is available online at <http://www.jasn.org/>.

Human	MSTASSSSSSSSSQTTPHPPSQMRRSAAAGSPFAVAAAGSGNGAGGGGGVGCAPAAGAGRL
Mouse	MSTASSSS-----SQTPHSAPQMRRS TAGSP--AAAGSGTGPAG-----SCAPAAGAGRL
Zebrafish	MSASPVHS-----ARVRRSNDGSPINTSSSASSS-----SSSSTGNTSR
Human	LQPIRATVPYQLLRGSQHSPTRPVAAA-----AASLGSLPGPGAARGPS PSSPTPPAA
Mouse	LQPIRATVPYQLLRGSQHSPTRPAAAAAT-----AAAALGSLSGPGGARGPS PSSPTPPA
Zebrafish	LQPIRATVPYQLLRGNQHSPTREPASFSTPSSSSSI SVGSNTEPTASAQHSNSTPGSETL
Human	AAPAEQAP---RAKGRPRRSPESHRRSSSPERRSPGSPVCR-ADKAKSQVRTSSTIRRT
Mouse	AAPAEQAP---RAKGRPRRSPESRRSSSPERRSPGSPVCR-VDRPKSQHIRTSSTIRRT
Zebrafish	ASPAGSASLDGRLIPRQRSPPEHR--SSPER-CPHSFVLAVERSKSQVVRTGAIARRT
Human	SSLDTITGPYLTGQWPRDPHVHYPSCKDKATQTPSCWAEEGA EKRS-HQRSASWGSADQ
Mouse	SSLDTITGPYLTGQWPRDPHVHYPSCKMRDKATQTPSCWAEEGA EKRS-HQRSASWGSADQ
Zebrafish	SSLGAIITGPYLIGQWPRESHLNPLCMKDKSTQTPGCWSESEEKRSTHQRSASWGSADH
Human	LKEQIAKLRLQQRSKQSS-RHSKE-KDRQSPHGNHITISHTQATG-----SRS
Mouse	LKE-IAKLRLQQRSKQSS-RHSKE-KDRQSPHGNHITISHTQAIG-----SRS
Zebrafish	LKE-IAKLRLQQRNKQGGGRQCKDSKECLSPHCCSTTTTITATTISTASQAPSSMSKS
Human	VMPLSNISVPKSSVSRVPCNVEGISPELEKVFIKENNGKEEVSKPLDIPDGRRAPLPAH
Mouse	VMPLSNISVPKSSVSRVPCNVEGISPELEKVFIKENNGKEEVSKPLDIPDGRRAPLPAH
Zebrafish	AQMPLSNITVPKPSISRVPSSMEGINHELEKVFIKDNGEKEEL-KALEVPDGRRAPFPQ
Human	YRSSSTRSIDTQTPSVQERSSSCSSHSPCVSPFCPPESQDGSPCSTEDLLYDRDKD SGSS
Mouse	YRSSSTRSIDTQTPSVQERSSSCSSHSPCVSPFCPPESQDGSPCSTEDLLYDRDKD SGSS
Zebrafish	QRSSSSRGIDTQTPSVQGRSSSCSSLSPCPS PACPPRSHDGSFYSTDEMLDDRDKD SGSS
Human	SPLPKYASSPKPNNSYMFKRE PPEGCERVKVFEE MASRQPI SAPLFSCPDKNKVNFIPTG
Mouse	SPLPKYASSPKPNNSYMFKRE PPEGCERVKVFEE MASRQPI SAPLFSCPDKNKVNFIPTG
Zebrafish	SPLPKFASSPKPNNSYMFKRE PPEGCEKIKVFEEMTSRQSTTVPLFSCPDKNKVNFIPTG
Human	SAFCPVKLLGPLL PASDMLKNSPNSGQSSALATLTVEQLSSRVSFTSLSDDTSTAGSME
Mouse	SAFCPVKLLGPLL PASDMLKNSPNSGQSSALATLTVEQLSSRVSFTSLSDDTSTADSLE
Zebrafish	SAFCPVKLPGSM LQHS SSQDEERE-PTQAGPSALHHMPTQVSTSTSTDDP-----
Human	ASVQQPSQQQQLLQELQGEDHISAQNYVVI
Mouse	PSAQQPSQQQQLLQDLQVEEHVSTQNYVMI
Zebrafish	--PESPSQQ---QEAPSESGSQPNFEVS

Supplementary Figure.1

Alignment of amino acid sequences of human, mouse and zebrafish Glcci1 predicted from their nucleotide sequences. The amino acid same with human, mouse and zebrafish are marked by shading.

Supplementary Table 1. Identification of protein sequences in peptides obtained from the 70 kDa and 150 kDa protein fractions in the urine of proteinuric zebrafish embryos using mass spectrometry sequencing. Only the 10 most prominent peptide sequences identified in each fraction are shown.

A. 150 kDa fraction		
<u>Accession</u>	<u>Protein name</u>	<u>Hits</u>
Q1LWN5_DANRE	Novel protein similar to vitellogenin 1 Vg1 Flags Fragment	420
A2VCZ6_DANRE	Zgc 136383 protein Flags Fragment	433
Q1LWN2_DANRE	Vitellogenin 1	383
Q1LWN4_DANRE	Novel protein similar to vitellogenin 1 Vg1 Flags Fragment	328
Q90YN8_DANRE	Vitellogenin 1	369
Q8JH37_DANRE	Vitellogenin 1 Flags Fragment	294
Q1LWN1_DANRE	Novel protein similar to vitellogenin 1 Vg1 Flags Fragment	294
A8WGJ7_DANRE	Zgc 136383 protein Flags Fragment	315
A4VCF4_DANRE	Vtg1 protein Flags Fragment	240
A3KMS4_DANRE	Vtg7 protein	269
B. 70 kDa fraction		
<u>Accession</u>	<u>Protein name</u>	<u>Hits</u>
Q1LWN5_DANRE	Novel protein similar to vitellogenin 1 Vg1 Flags Fragment	586
A2VCZ6_DANRE	Zgc 136383 protein Flags Fragment	597
Q1LWN2_DANRE	Vitellogenin 1	557
Q90YN8_DANRE	Vitellogenin 1	535
Q1LWN4_DANRE	Novel protein similar to vitellogenin 1 Vg1 Flags Fragment	473
Q8JH37_DANRE	Vitellogenin 1 Flags Fragment	385
Q1LWN1_DANRE	Novel protein similar to vitellogenin 1 Vg1 Flags Fragment	380
A4VCF4_DANRE	Vtg1 protein Flags Fragment	330
Q1MTC6_DANRE	Novel protein similar to vitellogenin 1 Vg1	422
Q1MTC4_DANRE	Novel protein similar to vitellogenin 1 Vg1	244

Supplementary Table 2. Identification of protein sequences in peptides obtained from the 70 kDa and 150 kDa protein fractions in the serum of adult wild type zebrafish using mass spectrometry sequencing. Only the 10 most prominent peptide sequences identified in each fraction are shown.

A. 150kDa fraction

Accession	Protein name	Hits
IPI00508594	vtg1;vtg5 Vitellogenin 1	228
IPI00919379	vtg7 149 kDa protein	215
IPI00975348	vtg7 149 kDa protein	223
IPI00858854	vtg6 vitellogenin 6	209
IPI00866006	vtg7 Vtg7 protein	191
IPI00920458	vtg7 124 kDa protein	157
IPI00503804	vtg3 vitellogenin 3, phosvitinless	67
IPI00500668	vtg2 Novel protein similar to vitellogenin 1	62
IPI00615908	Novel protein similar to complement component 3	42
IPI00506519	cp Ceruloplasmin	49

B. 70kDa fraction

Accession	Protein name	Hits
IPI00972722	tfa Transferrin	154
IPI00505602	Complement component c3b	56
IPI00773000	fetub fetuin B	54
IPI00513243	lmnb2 Lamin B2	39
IPI00835213	si:dkey-76b14.4 185 kDa protein	41
IPI00963174	si:dkey-76b14.4 Novel protein	40
IPI00864674	191 kDa protein	34
IPI00975348	vtg7 149 kDa protein	21
IPI00858854	vtg6 vitellogenin 6	20
IPI00866006	vtg7 Vtg7 protein	21